Atmos. Chem. Phys. Discuss., 6, 5387–5425, 2006
www.atmos-chem-phys-discuss.net/6/5387/2006/

Atmospheric Chemistry and Physics Discussions

Comparisons between SCIAMACHY atmospheric CO_2 retrieved using (FSI) WFM-DOAS to ground based FTIR data and the TM3 chemistry transport model

M. P. Barkley[1], **P. S. Monks**[2], **U. Frieß**[1,*], **R. L. Mittermeier**[3], **H. Fast**[3], **S. Körner** [4], **and M. Heimann** [4]

[1]EOS, Space Research Centre, Department of Physics & Astronomy, University of Leicester, Leicester, UK
[2]Department of Chemistry, University of Leicester, Leicester, UK
[3]Meteorological Service of Canada (MSC), Downsview, Ontario, Canada
[4]Max Planck Institute for Biogeochemistry (MPI-BGC), Jena, Germany
[*]Present address Institute of Environmental Physics, Heidelberg, Germany

Received: 20 April 2006 – Accepted: 16 May 2006 – Published: 27 June 2006

Correspondence to: P. S. Monks (psm7@le.ac.uk)

Abstract

Atmospheric CO_2 concentrations, retrieved from spectral measurements made in the near infrared (NIR) by the SCIAMACHY instrument, using Full Spectral Initiation Weighting Function Modified Differential Optical Absorption Spectroscopy (FSI WFM-DOAS), are compared to ground based Fourier Transform Infrared (FTIR) data and to the output from a global chemistry-transport model.

Analysis of the FSI WFM-DOAS retrievals with respect to the ground based FTIR instrument, located at Egbert, Canada, show good agreement with an average negative bias of approximately −4.0% with a standard deviation of ∼3.0%. This bias which exhibits an apparent seasonal trend, is of unknown origin, though slight differences between the averaging kernels of the instruments and the limited temporal coverage of the FTIR data may be the cause. The relative scatter of the retrieved vertical column densities is comparable to the spread of the FTIR measurements themselves. Normalizing the CO_2 columns using the surface pressure does not affect the magnitude of this bias although it slightly increases the scatter of the FSI data.

Comparisons of the FSI retrievals to the TM3 global chemistry-transport model, performed over four selected Northern Hemisphere scenes show good agreement. The correlation, between the time series of the SCIAMACHY and model monthly scene averages, are ∼0.7 or greater, demonstrating the ability of SCIAMACHY to detect seasonal changes in the CO_2 distribution. The amplitude of the seasonal cycle, peak to peak, observed by SCIAMACHY however, is overestimated by a factor of 2–3, which cannot be explained. The yearly means detected by SCIAMACHY are within 2% of those of the model with the mean difference between the CO_2 distributions also approximately 2.0%. Additionally, analysis of the retrieved CO_2 distributions reveals structure not evident in the model fields which correlates well with land classification type.

From these comparisons, the overall precision and bias of the CO_2 columns retrieved by the FSI algorithm are estimated to be close to 1.0% and <4.0% respectively.

1 Introduction

Carbon dioxide (CO_2) is the dominant anthropogenic greenhouse gas whose rapid 30% increase in the last 200 years has caused an enhancement in the radiative forcing of the Earth's atmosphere (Intergovernmental Panel on Climate Change, 2001). The growth in atmospheric CO_2 levels is attributed primarily to the burning of fossil fuels and land use change with the present concentration far exceeding anything previously over the last 650 000 years (Siegenthaler et al., 2005). Two important sinks which control the amount of CO_2 in the atmosphere are the terrestrial biosphere and the ocean, which have been estimated to have absorbed approximately half of the anthropogenic emissions (Sabine et al., 2004). Understanding the response of both these sinks and of the carbon cycle as a whole, to escalating atmospheric CO_2 levels and global warming is essential for predicting future climate change, especially as feedback mechanisms within the cycle are still not fully understood (see Friedlingstein et al., 2003, and references therein).

Whilst much effort has gone into estimating carbon cycle fluxes using chemistry transport models and inverse methods, their distribution and magnitudes can still only be made at continental and ocean basin scales (Gurney et al., 2002). To place tighter constraints on the models, more observations of the atmospheric CO_2 distribution are needed to complement those supplied by the sparse network of NOAA/CMDL ground stations. Satellite measurements can, in principle, provide the dense sampling needed. However, the low spatial and temporal gradients associated with atmospheric CO_2 require measurements to be made accurately and to a high precision to be of any value. To improve over the existing ground network monthly averaged column data, at a precision of 1% (2.5 ppmv) or better, for an $8^{\circ} \times 10^{\circ}$ footprint are needed (Rayner and O'Brien, 2001), although regionally this threshold can be relaxed (Houweling et al., 2004).

Recent efforts utilizing the thermal infrared, for example using the NOAA-TOVS (Chédin et al. 2002, 2003) or AIRS instruments (Chevallier et al., 2005; Chahine et al.,

2005) and the adjacent near infrared, using SCIAMACHY (Buchwitz et al., 2005b), have demonstrated that we are entering an era where satellite monitoring of atmospheric CO_2 concentrations are becoming a feasible prospect. Such research together with future missions such as the Greenhouse gases Observing Satellite (GOSAT) (http://www.jaxa.jp/missions/projects/sat/eos/gosat) and Orbiting Carbon Observatory (OCO) (Crisp et al., 2004), may yield additional knowledge about the CO_2 surface fluxes. However, if satellite observations are to provide information about carbon cycle processes then they require careful validation. In the future this will be primarily achieved using a new network of ground-based near-infrared Fourier Transform Infrared (FTIR) spectrometers, currently under construction, called the Total Carbon Column Observing Network (TCCON) (Wennberg et al., 2005). At present though, such comparison efforts are limited to a handful of FTIR ground stations (e.g. Dils et al., 2006) and, or alternatively to, chemistry transport models (e.g. Buchwitz et al., 2005a).

In this work, atmospheric CO_2 vertical columns retrieved from SCIAMACHY NIR measurements using a new algorithm called Full Spectral Initiation (FSI) WFM-DOAS are compared both to FTIR measurements and to a global chemistry-transport model to ascertain the quality and accuracy of the retrieval method. The ability of the FSI algorithm to detect temporal and spatial variations in the CO_2 distribution is also assessed. In Sects. 2 and 3 the SCIAMACHY instrument and the retrieval algorithm are summarized. Comparisons to the FTIR data and to the model data are then made in Sects. 4 and 5 respectively. Retrieval errors and precision are discussed in Sect. 6 and an overall summary is given in Sect. 7.

2 The SCIAMACHY instrument

Launched onboard the ENVISAT satellite, in March 2002, the SCanning Imaging Absorption spectroMeter for Atmospheric CHartographY (SCIAMACHY) instrument is a passive UV-VIS-NIR hyper-spectral spectrometer designed to investigate tropospheric and stratospheric composition and processes (Bovensmann et al., 1999). The instru-

ment measures sunlight that is reflected from or scattered by the atmosphere, covering the spectral range 240–2380 nm (non-continuously) using eight separate grating spectrometers (or channels). The spectral resolution varies between channels (0.2–1.4 nm) with each channel consisting of 1024 diode detectors, with each detector pixel sampling at about half the full-width half-maximum (FWHM) for a given channel. For the majority of its near polar sun-synchronous orbit SCIAMACHY makes measurements of the atmosphere in an alternating limb-nadir sequence. In addition the solar irradiance and lunar radiance are measured using solar/lunar occultation. The vertical column densities (VCDs), (units of molecules cm^{-2}), of various trace gases, whose absorption features lie within SCIAMACHY's spectral range, can then be determined through the inversion of the logarithmic ratio of the earthshine radiance and solar irradiance via differential absorption spectroscopy (DOAS), (Platt, 1994). In this analysis, atmospheric CO_2 distributions are determined by retrieving CO_2 VCDs from nadir observations made in the NIR, focussing on a small micro window within channel six, centered on the CO_2 band at 1.57 μm. A characteristic set of observations consists of the nadir mirror scanning across track for 4 s followed by a fast 1 s back-scan. This is repeated for either 65 or 80 s according to the orbital region. The ground swath viewed has a fixed dimensions of $960 \times 30\,km^2$, (across × along track). For channel 6, the nominal size of each pixel within the swath is $60 \times 30\,km^2$, corresponding to an integration time of 0.25 s. Global coverage is achieved at the Equator within 6 days.

3 Full Spectral Initiation (FSI) WFM-DOAS

The Full Spectral Initiation (FSI) WFM-DOAS retrieval algorithm, discussed in detail in Barkley et al. (2006), has been developed specifically to retrieve CO_2 from space using SCIAMACHY measurements made in the NIR. It is an extension of the WFM-DOAS algorithm first introduced by Buchwitz et al. (2000) which has been used to retrieve the VCDs of a variety of trace gas species, from different spectral intervals, including CO_2, methane (CH_4) and carbon monoxide (CO) from the NIR (Buchwitz et al. 2004,

2005b); water vapour (H_2O) from the near-visible (Nöel et al., 2004) and ozone (O_3) from the UV (Coldewey-Egbers et al., 2005).

The algorithm, defined in Eq. (1), is based on a linear least squares fit of the logarithm of a model reference spectrum I_i^{ref} and its derivatives, plus a quadratic polynomial P_i, to the logarithm of the measured sun normalized intensity I_i^{meas}.

$$\left\| \ln I_i^{\text{meas}}(\mathbf{V}^t) - \left[\ln I_i^{\text{ref}}(\bar{\mathbf{V}}) + \sum_j \frac{\partial \ln I_i^{\text{ref}}}{\partial \bar{V}_j} \cdot (\hat{V}_j - \bar{V}_j) + P_i(a_m) \right] \right\|^2 \equiv \|\text{RES}_i\|^2 \;\rightarrow\; \min \;\; \text{w.r.t } \hat{V}_j \;\&\; a_m \tag{1}$$

The subscript i refers to each detector pixel of wavelength λ_i and the true, model and retrieved vertical columns are represented by $\mathbf{V}^t = (V^t_{CO_2}, V^t_{H_2O}, V^t_{\text{Temp}})$, $\bar{\mathbf{V}} = (\bar{V}_{CO_2}, \bar{V}_{H_2O}, \bar{V}_{\text{Temp}})$ and $\hat{V}_j$ respectively (where subscript j refers to the variables CO_2, H_2O and temperature). Here V_{Temp} is not a vertical column as such, but rather a scaling factor applied to the vertical temperature profile. Each derivative (or column weighting function) represents the change in radiance as a function of a relative scaling of the corresponding trace gas or temperature profile. To retrieve carbon dioxide, weighting functions for CO_2, H_2O and temperature are needed, thus the fit parameters are the trace gas VCDs, $\hat{V}_{CO_2}$ and $\hat{V}_{H_2O}$, the temperature scaling factor $\hat{V}_{\text{Temp}}$ and the polynomial coefficients a_m. The error associated with each of the retrieved variables is given by Eq. (2) where $(\mathbf{C_X})_{jj}$ refers to the j-th diagonal element from the least squares fit covariance matrix, RES_i is the fit residual, m is the number of spectral points within the fitting window and n is the number of fit parameters.

$$\sigma_{\hat{V}_j} = \sqrt{\frac{(\mathbf{C_X})_{jj} \times \sum_i \text{RES}_i^2}{(m-n)}} \tag{2}$$

Whilst initial results by Buchwitz et al. (2005b) are promising, a detailed error analysis, conducted by Barkley et al. (2006), showed that the error associated with the retrieved CO_2 VCD is significantly reduced when the reference spectrum (I_i^{ref}) is created from an a priori scenario that closely resembles the true conditions. Using this premise, the FSI algorithm differs from current implementations of WFM-DOAS in that rather than using a look-up table approach, it generates a reference spectrum for each individual SCIAMACHY observation, based on the known properties of the atmosphere and surface at the time of the measurement. As the calculation of radiances is computationally expensive, FSI is not implemented as an iterative scheme, rather each reference spectrum only serves as the best possible linearization point for the retrieval. Each spectrum is generated using the radiative transfer model SCIATRAN (Rozanov et al., 2002), using several different sources of atmospheric and surface data that serve as input, the details of which are only summarized here:

- A CO_2 vertical profile is selected from a climatology, prepared by J. Remedios (University of Leicester, private communication, 2005), according to the time of the observation and the latitude band in which the ground pixel falls.
- Temperature, pressure and water vapour profiles, derived from operational 6 hourly ECMWF data (1.125°×1.125° grid), are interpolated onto the local overpass time and centre of the of the ground pixel.
- From using the mean radiance (within the fitting window) of the SCIAMACHY observation and the solar zenith angle at the corresponding time, it is possible to infer an approximate value for the surface albedo by comparing it to radiances in a pre-constructed look-up table (generated as a function of the surface reflectance and solar zenith angle).
- Aerosols have already been discovered to cause systematic errors in SCIAMACHY CO_2 columns (Houweling et al., 2005). To account for this three aerosol scenarios are incorporated into the retrieval algorithm. Maritime, rural and urban

scenarios are implemented over the oceans, land and urban areas respectively using the LOWTRAN aerosol model (Kneizys et al., 1996).

The FSI algorithm is applied to radiances, corrected for dark current and non-linearity (see Kleipool, 2003a and Kleipool, 2003b, respectively), using the fitting window 1561.03–1585.39 nm, which contains ~32 detector pixels. The SCIAMACHY dead and bad (DBM) pixel mask which flags corrupt detector pixels is updated each orbit using the standard deviations of the dark current, as proposed by Frankenberg et al. (2005). Detector pixels are also discarded if erroneous spikes occur in the measured radiance. The algorithm also uses a solar spectrum with improved calibration in preference to that in the official SCIAMACHY product (v5.04), provided by ESA, courtesy of J. Frerick (ESA, ESTEC). To improve the quality of the FSI spectral fits, the latest version of the HITRAN molecular spectroscopic database (Rothman et al., 2005) has been implemented in SCIATRAN .

All SCIAMACHY observations are cloud screened prior to retrieval processing, with cloud contaminated pixels flagged and disregarded. The latest version of the FSI algorithm (v1.2) uses the cloud detection method devised by Krijger et al. (2005), though it should be noted that some scenes (processed using FSI v1.1) were screened using the Heidelberg Iterative Cloud Retrieval Utilities (HICRU) database (Grzegorski et al., 2005). Back-scans along with observations that have solar zenith angles greater than 75° are also excluded. Pixels over the oceans (in this study) are also not processed owing to the low surface reflectivity, which often results in SCIAMACHY spectra with a poor signal to noise ratio. Each retrieved CO_2 VCD is normalized using the input ECMWF surface pressure to produce a vertical column volume mixing ratio (VMR). After retrieval processing, a quite strict quality filter is applied selecting only those VMRs that have retrieval errors less than 5% and are within the range 340–400 ppmv. Unlike other studies, e.g. Buchwitz et al. (2005a, 2005b) or Yang et al. (2002), adjustment of the VCD or VMR magnitudes, via scaling factors, has not been necessary.

The advantage of the NIR over the thermal infrared, is the sensitivity to the CO_2 concentration in the lowermost part of the troposphere. This is demonstrated by the

FSI averaging kernels (shown in Fig. 1) which peak in the planetary boundary layer at a maximum of 1.5. This indicates that the retrieved profile is over (under) estimated by 50% if its true form is greater (lower) than the reference profile therefore over (under) estimating the corresponding retrieved VCD accordingly (Buchwitz et al., 2005b). The averaging kernels decrease with altitude and above approximately 7 km they are less than 1.0 , i.e. less sensitive than at lower altitudes.

4 Comparisons to FTIR CO_2 measurements over Egbert, Canada

4.1 Methodology

In this analysis comparisons are made between columns retrieved by the FSI algorithm to CO_2 columns measured by the ground based (g-b) FTIR instrument, run by Environment Canada, located at the Centre of Atmospheric Research Experiments (CARE), Egbert, Canada (44.23° N–79.78° E). This station, chosen in preference to the high latitude station of Ny Alesund and high altitude instrument at Jungfraujoch, is located within a large rural area thus rendering it ideal for atmospheric measurements. Solar absorption spectra are recorded, in cloud free conditions, approximately twice each month using an ABB Bomen DA8 FTIR spectrometer that has an apodized resolution of 0.004 cm^{-1}. Measurements of the CO_2 VCD are derived from the recorded spectra, using two wavelength intervals 2625.35–2627.06 cm^{-1} and 936.44–937.18 cm^{-1}, to an accuracy of 8.9% (error estimate based on the discussion in Murphy et al., 2001).

The two data sets are compared for the year 2003, however during this time period there are only 74 g-b measurements but over five thousand SCIAMACHY valid retrievals (selected on the basis of being within ±10.0° longitude and ±2.5° latitude of the station). To ensure a meaningful analysis is performed, the methodology outlined by Dils et al. (2006) is used to compare the data. It is also assumed that the averaging kernels of the FTIR instrument (not yet available) and SCIAMACHY are very similar. First, both data sets are normalized to sea level altitude using a simplified hypsometric

formula given in Eq. (3), where C_z is the measured CO_2 VCD, Z (in metres) the corresponding average surface elevation of this observation (in the case of the station this is 251 m) and C_0 is the VCD normalized to sea-level. This calculation effectively removes any altitude effects that may be associated with either set of CO_2 measurements.

$$C_0 = C_z\left(\frac{Z}{7400.0}\right) \tag{3}$$

The second step is to fit a third order polynomial through the daily averaged FTIR g-b data so that each FSI VCD can be compared to a time-interpolated value of the resultant fit (PF). This is in preference to directly comparing the FSI retrievals to the actual FTIR data. The bias B_i, of each FSI column FSI_i, with respect to the time-interpolated polynomial PF_i is given by Eq. (4) with the bias for the year being simply the mean of this ensemble.

$$B_i = \left(\frac{\mathrm{FSI}_i - PF_i}{\mathrm{FSI}_i}\right) \tag{4}$$

Finally the scatter σ_{scat} of the FSI CO_2 VCDs can also be assessed using the $1\,\sigma$ deviation of their daily average $\mathrm{FSI}_{\mathrm{day}}$ with respect to the polynomial fit, providing they have been corrected for the associated daily bias, B_{day}.

$$\sigma_{\mathrm{scat}} = \mathrm{std}\left(\frac{\mathrm{FSI}_{\mathrm{day}} - (1 + B_{\mathrm{day}}) * PF_{\mathrm{day}}}{(1 + B_{\mathrm{day}}) * PF_{\mathrm{day}}}\right) \tag{5}$$

This procedure was then subsequently repeated but this time with FTIR data normalized with the ECMWF surface pressure (instead of Eq. 3), so that the g-b measurements could be compared to the corresponding final (normalized) FSI VMR product.

4.2 Results

During 2003 there were a total number of 5150 successful cloud free CO_2 FSI retrievals over the Egbert site. These are illustrated in Fig. 2a, together with the g-b FTIR VCD

measurements. The mean yearly bias of the FSI CO_2 columns with respect to the g-b data is -4.1%, with a standard deviation of 3.0% and scatter of 0.8%. These results are consistent with the WFM-DOAS results presented in Dils et al. (2006) who also reported a significant negative bias (Table 1), though in this analysis the mean bias is approximately half their reported value. The spread of the FSI retrievals is quite small (0.8%) when compared to the scatter of the FTIR data (1.3%).

Selecting a subset of the FSI CO_2 VCDs on the basis of being within only $\pm 5.0^{\circ}$ longitude and $\pm 2.5^{\circ}$ latitude of the station does not reduce this offset as it has a similar mean yearly bias of -4.0% and standard deviation of 3.0%. That said, the scatter was slightly larger at 1.3%. This negative bias is not constant throughout the year (Fig. 2b) exhibiting an apparent seasonal trend, with the significant correlation (0.97) between the magnitude of the FSI columns and their corresponding individual biases. This offset is at a maximum in July, where the FSI algorithm retrieves lower CO_2 columns than the FTIR instrument. This bias cannot be attributed to a solar zenith angle dependence as this is passed to the radiative transfer model when creating each reference spectrum.

Normalizing the CO_2 VCDs does not have a dramatic effect only slightly increasing the bias on both grids by about 0.2%, though the scatter does become almost twice as great. The perceptible seasonal trend however, is not removed from the monthly biases. The origin of this bias and its seasonal variation has not been identified. Differences between the SCIAMACHY and FTIR averaging kernels may account for some of the negative bias whilst the limited number of the g-b measurements may partly explain its temporal evolution. Nevertheless, this bias does decreases rapidly in the latter months of 2003, thus a more comprehensive set of FTIR observations for 2004 is required to see if this seasonal pattern is repeated.

ACPD
6, 5387–5425, 2006

5 Comparisons to the TM3 chemistry transport model

5.1 The TM3 chemical transport model

The TM3 is a global atmospheric tracer model, developed by the Max Planck Institute for Biogeochemistry (MPI-BGC), which solves the continuity equation for an arbitrary number of atmospheric tracers (Heimann and Körner, 2003). The atmospheric transport is driven by National Center for Environmental Prediction (NCEP) meteorological fields using a model grid of 1.8°×1.8°×29 layers (although its initial ten year start-up run is at a coarser resolution of 4°×5°×19 layers). The ocean air-sea fluxes are based on the monthly pCO_2 climatology compiled by Takahashi et al. (2002) whilst the natural terrestrial biospheric fluxes were modeled using the BIOME-BGC model driven with daily NCEP data, using a simple diurnal cycle algorithm (Thornton et al., 2005). Anthropogenic fossil fuel CO_2 emissions are derived from the EDGAR 3.2 database (Olivier and Berdowski, 2001) linearly extrapolated from the years 1990 and 1995. The model includes biomass burning estimates (at monthly resolution) taken from van der Werf et al. (2003), but it does not account for the temporal behaviour of fossil fuel emissions.

The TM3 CO_2 VMRs have been calibrated for an optimal match with in-situ observations made at the South Pole station and with a mean FSI averaging kernel (shown in Fig. 1) applied to the model data to account for the increased sensitivity of SCIAMACHY to the lower part of the troposphere. The model has been sampled at the exact location and time (using the model's closest 3 hourly time step) for each FSI retrieved CO_2 column that has passed the quality filter. Both data sets have then been averaged onto a 1°×1° grid with the temporal and spatial behaviour of the CO_2 distributions then examined.

In this paper comparisons are made for four specific regions: Siberia and Canada/Alaska (hereafter referred to as the North American scene), the Gobi desert and Western Europe (Fig. 4). Both Siberia and North American are covered extensively by boreal forests and Arctic tundra and should exhibit a strong seasonal cycle due to the uptake and release of CO_2 by vegetation. The CO_2 distribution over the

Gobi desert should instead be more influenced by atmospheric transport from other regions whilst over Western Europe, both aerosols and pollution are expected to have a greater effect.

To assess the accuracy of the model data a similar comparison to the g-b measurements was also performed. The TM3 data shows excellent agreement to the FTIR data having a negative bias of only 2% with minimal scatter (Table 1 and Fig. 2). However, as with the FSI retrievals, the monthly bias associated with the TM3 data (Fig. 3) also demonstrates a seasonal trend, although less pronounced.

5.2 Time series comparisons

The temporal behaviour of CO_2 VMRs over the Siberian region are illustrated in Fig. 5a, with the time series plot of the monthly averages demonstrating that there is quite good agreement between the model and the FSI algorithm. The correlation coefficient between the two time series is 0.75 and the TM3 monthly means lie within the FSI error limits for all but the summer months. The most noticeable difference is that whilst during the winter months there is excellent agreement between the model and observations, during the rest of the year SCIAMACHY detects lower CO_2 VMRs. The yearly average of the absolute difference is 7.3 ppmv (2%) with the mean of the standard deviations (of the monthly differences) being 7.6 ppmv (see Table 2). The mean CO_2 VMR for the whole year detected by SCIAMACHY is 371.2 ppmv whereas the model average is 377.5 ppmv. This suggests a negative bias between the model and FSI retrievals of about ~2.0% (relative to the FSI scene mean).

The amplitude of the seasonal cycle (peak to peak) of 20.7 ppmv detected by SCIAMACHY is just under three times that of the model (7.9 ppmv) with both time series agreeing on the timing of the minimum CO_2 VMR in July, though disagreeing on the occurrence of the maximum (April for the TM3 and January for SCIAMACHY). Similar results were presented by Buchwitz et al. (2005a) who reported a factor of four greater amplitude. Inspecting the time series of the CO_2 anomaly shows that the transition from positive to negative, as biospheric photosynthesis exceeds respiration, begins

slightly earlier for the FSI data (late April) than the model (early May). Both data sets agree on the return crossover in mid-October.

Examining the North American scene reveals many similarities to the Siberian region. There is quite high correlation (0.67) between the time series of the monthly averages (Fig. 5b) and both SCIAMACHY and model agree on the timing of the minimum CO_2 VMR (in July) though differ on the occurrence of the maxima. The yearly averages are 371.6 ppmv (FSI) and 377.5 ppmv (TM3) with the amplitude of the seasonal cycle observed by SCIAMACHY being just over twice that of the model (15.4 ppmv as opposed to 7.0 ppmv). In addition, the mean of the absolute monthly differences is 6.0 ppmv (1.6%), with the mean of the standard deviations being 7.9 ppmv. This difference is slightly smaller than found for the Siberian region, even though the actual FSI retrieval errors are a fraction greater. Like its Siberia counterpart the FSI CO_2 anomaly appears to be out of phase with that of the model with each transition occurring approximately one month earlier, indicating that SCIAMACHY is observing the same seasonal variation for both of these (very similar) scenes.

Over Western Europe (Fig. 6a), model and observations agree less well reflecting the greater difficulty of retrieving over this region (owing to pollution events and aerosols potentially affecting the light path (Houweling et al., 2005)). Whilst the amplitude of the observed seasonal cycle is only just over a factor of two larger than the model there is little coherence between the time series with a correlation of only 0.47 and an average (absolute) difference of ~3% or more. In contrast, over the Gobi Desert (Fig. 6b), the match between the TM3 model data and the retrieved CO_2 VMRs is excellent with the correlation between the time series now being 0.95 and with both agreeing on the timing of the maximum (April) and minimum (July) CO_2 VMR. The CO_2 anomalies are thus in phase and the small difference between yearly means, 374.0 ppmv (FSI) and 377.3 ppmv (TM3) (about 1%), is most likely due to the increased signal to noise ratio produced by the high albedo of the desert surface. In spite of the better agreement, SCIAMACHY still detects a seasonal signal, transported from other regions, which is just over twice that of the TM3 data (10.1 ppmv to 4.9 ppmv). It should also be noted

that the higher CO_2 VMRs, falsely created by dust and aerosols, detected by Houweling et al. (2005), over the Saharan Desert are not evident in FSI retrievals over the Gobi Desert.

5.3 Spatial distribution

Close inspection of the model fields reveal that they are much smoother and contain far less variability than those observed by SCIAMACHY. Over the Gobi Desert and Western Europe, i.e. the smaller scenes, coincidental features are difficult to identify, nevertheless Fig. 7 is a rare example where both SCIAMACHY and the model data agree on lower CO_2 concentrations over the Netherlands, Denmark and Northern Germany.

For the larger scenes, e.g. North America, more structure is visible within the SCIAMACHY data as Fig. 8 clearly shows an evolving CO_2 distribution, irrespective of some of the high degree of variation between grid boxes. For example, a large CO_2 enhancement, in the SCIAMACHY data, over Ellesmere Island and the north-western edge of Greenland is easily noticeable in April (Fig. 9). The best spatial agreement over the North American scene is in June, when lower CO_2 concentrations over Québec and the Labrador Coast and also diagonally through the central regions of Canada, are evident in both model and observations.

During July however, an apparently massive uptake of CO_2 is detected by SCIAMACHY over the area around and to the west of Hudson Bay (the Canadian Shield), that is not predicted by the model (though this uptake needs to be deconvolved from any possible seasonal bias). This feature, not believed to be a residual surface reflectance effect (as an a priori albedo value is used within the FSI algorithm) is not visible in May but seemingly develops thorough the summer before disappearing by October. The Great Central Plains immediately adjacent to the west of Canadian Shield do not demonstrate this variation, suggesting that the Canadian Shield is an active carbon sink. Comparison of the land vegetation type, taken from the MODIS land ecosystem classification product and re-gridded to $1^{\circ}\times1^{\circ}$, shows that the transition from low CO_2

concentrations to higher values, across from the Canadian Shield to the Great Central Plains, corresponds to a change in vegetation type from evergreen needle leaf and mixed forests to land covered by crops and large grass plains (Fig. 10). Is it possible that SCIAMACHY is witnessing greater uptake of atmospheric CO_2 by the forests compared to the farmed regions? This is difficult to clarify but this distinct feature is missed by the TM3 model thus highlighting the exciting potential (and use) of SCIAMACHY to detect sub-continental carbon sources and sinks at the surface. This is also demonstrated by SCIAMACHY observations over Siberia. For example in October, the model output is very uniform whilst SCIAMACHY sees an enhancement approximately along the Yenisey River (which splits the West Siberian Plain and the Central Siberian Plateau (Fig. 11). Similarly in May, the large CO_2 VMRs seen over the Yablononvyy mountain range (approximately 115° E 49° N) are not discernible in the model.

Thus, while SCIAMACHY captures the overall temporal behaviour of the model CO_2 distributions well, as described in Sect. 5.2, the spatial coherence between the data sets is less favourable. This is further indicated by the time series of the linear correlation coefficient (Figs. 5 and 6) which typically stays below 0.5 in all regions and is even negative for some months, signifying that observed and model CO_2 distributions are anticorrelated.

6 Retrieval errors and precision

It is important to give some assessment of the accuracy (bias) and precision of the CO_2 VMRs retrieved by the FSI algorithm. The mean retrieval (spectral fitting) errors over North America and Siberia are 2.88% and 2.70% respectively, whilst over Western Europe and the Gobi Desert they are 2.58% and 1.92% (see Table 3). These fit errors are predominantly affected by the signal to noise ratio of the spectra and thus are strongly influenced by the surface albedo which over the selected scenes, with exception of the Gobi Desert, is quite low (typically below 0.1). The standard deviation of the "raw" (un-gridded) FSI CO_2 columns is ~3.0% which seems consistent with the

mean retrieval errors. That said, some of this spread can also be attributed to scattering from aerosols and undetected clouds. The mean of the standard deviations, of the retrieval errors over each scene, is consistently below 1% implying that FSI spectral fitting procedure is itself quite precise. The mean root mean square (RMS) error of the spectral fits is also extremely stable at 0.1–0.3%.

The precision error in the monthly scene averages is given by $\sqrt{(\sigma/N)}$, where σ is the standard deviation of the scene mean and N the number of TM3 grid points used in its calculation. For all but the some of the winter months this precision error is also consistently below 1%.

It is difficult to estimate the bias of the retrieval using FTIR data from only a single ground station. The normalized CO_2 columns retrieved over the Egbert instrument have a negative average monthly bias of approximately −4.0%, although this does vary seasonally and decreases dramatically towards the end of 2003. Without comparisons to other column measurements made at other locations it is impossible to determine wether this bias is consistent globally or intrinsic only to the Egbert station. However, comparisons of the FSI retrievals to the TM3 data suggest a negative bias of about −2% with respect to the model, which when coupled with the −2% bias of the TM3 data to the FTIR measurements themselves (Sect. 5.1), implies that a bias of −4% to the true CO_2 concentration is probably realistic (assuming both the FTIR and model data are correct). As both the FSI retrievals and the model monthly biases show a seasonal trend (Fig. 3), it is hard to establish if a definite seasonal bias exists within the FSI algorithm. The lower concentrations observed (in all regions) during the summer months, relative to the model data, however does indicate that SCIAMACHY is possibly underestimating the CO_2 distributions in this time period.

7 Conclusions

Atmospheric CO_2 VMRs have been successfully retrieved from SCIAMACHY measurements in the NIR using the FSI retrieval algorithm with comparisons to both ground

based FTIR data and to the TM3 global chemistry transport model also performed.

With respect to the measurements made by the Egbert FTIR station, the yearly bias and its standard deviation of the FSI CO_2 VCDs are found to be approximately −4.1% and 3.0% respectively, with the relative scatter comparable to the scatter of ground-based measurements themselves. Inspection of the average monthly biases reveal an apparent seasonal trend, the cause of which has not been established. Normalizing the FTIR VCDs with the surface pressure does not remove this bias or its seasonal variation. Intermittent observations by the FTIR instrument and differences between its averaging kernel and that of SCIAMACHYs may partly be responsible for these dissimilarities.

Comparisons between the CO_2 fields predicted by the TM3 model and those observed by SCIAMACHY over four selected scenes show, in general, good agreement. The yearly average of the scenes is detected to within 2% with the mean difference between the CO_2 distributions being 1–3% and the mean of the standard deviations approximately 2%. The correlation between the time series of the SCIAMACHY and TM3 monthly scene averages is typically ≈0.7 or greater demonstrating the ability of the FSI algorithm to retrieve seasonal changes in CO_2 concentrations. However, irrespective of the region investigated, SCIAMACHY detects a seasonal cycle amplitude that is about 2–3 times larger than predicted by the model, which cannot as yet, be explained.

In addition, SCIAMACHY has observed interesting features within CO_2 distributions that are not predicted by the model. Future research will focus on these spatial structures, investigating possible links between areas of CO_2 uptake to vegetation net primary production and areas of enhanced CO_2 from biomass burning events.

From this study the overall precision and bias of the retrieved columns are estimated to be close to 1.0% and <4.0% respectively. It also must be re-stressed that at no stage whatsoever have scaling factors been applied to the FSI retrieved CO_2 VMRs as they have been in other studies. Whilst these results are encouraging they are still not of the desired quality for inverse modelling. It is hoped that further improvements

to the retrieval algorithm, through better calibration of the SCIAMACHY data and by improving the quality of the input a priori data used in the creation of the reference spectra, will overcome this issue in the future.

Acknowledgements. The authors would like to thank all those involved with the SCIAMACHY instrument especially J. Burrows and the team at IUP/IFE Bremen. We are also grateful to M. Grzegorski for providing the HICRU cloud data and A. Rozanov for supplying the radiative transfer model SCIATRAN. We would like to thank ESA for supplying the SCIAMACHY data, all of which was processed by DLR, and the British Atmospheric Data Centre (BADC) for supplying the ECMWF operational data set. The authors finally wish to thank both the Natural Environment Research Council (NERC) and CASIX (the Centre for observation of Air-Sea Interactions and fluXes) for supporting M. Barkley through grant ref: NER/S/D/200311751.

References

Barkley, M. P., Frieß, U., and Monks, P. S.: Measuring atmospheric CO_2 from space using Full Spectral Initiation (FSI) WFM-DOAS, Atmos. Chem. Phys. Discuss., 6, 2765–2807, 2006. 5391, 5393

Bovensmann, H., Burrows, J. P., Buchwitz, M., Frerick, J., Nöel, S., Rozanov, V. V., Chance, K. V., and Goede, A.: SCIAMACHY mission objectives and measurement modes, J. Atmos. Sci., 56, 127–150, 1999. 5390

Buchwitz, M. and Burrows, J. P.: Retrieval of CH_4, CO, and CO_2 total column amounts from SCIAMACHY near-infrared nadir spectra: Retrieval algorithm and first results, in: Remote Sensing of Clouds and the Atmosphere VIII, Proceedings of SPIE, edited by: Schäfer, K. P., Comèron, A., Carleer, M. R., and Picard, R. H., 5235, 375–388, 2004. 5413

Buchwitz, M., Rozanov, V. V., and Burrows, J. P.: A near infrared optimized DOAS method for the fast global retrieval of atmospheric CH_4, CO, CO_2, H_2O, and N_2O total column amounts from SCIAMACHY/ENVISAT-1 nadir radiances, J. Geophys. Res., 105, 15 231–15 246, 2000. 5391

Buchwitz, M., de Beek, R., Bramstedt, K., Nöel, S., Bovensmann, H., and Burrows, J. P.: Global carbon monoxide as retrieved from SCIAMACHY by WFM-DOAS, Atmos. Chem. Phys., 4, 1945–1960, 2004. 5391

Buchwitz, M., de Beek, R., Burrows, J. P., Bovensmann, H., T.Warneke, Notholt, J., Meirink, J. F., Goede, A. P. H., Bergamaschi, P., Körner, S., Heimann, M., and Schulz, A.: Atmospheric methane and carbon dioxide from SCIAMACHY satellite data: initial comparison with chemistry and transport models, Atmos. Chem. Phys., 5, 941–962, 2005a. 5390, 5394, 5399

Buchwitz, M., de Beek, R., Nöel, S., Burrows, J. P., Bovensmann, H., Bremer, H., Bergamaschi, P., Körner, S., and Heimann, M.: Carbon monoxide, methane and carbon dioxide columns retrieved from SCIAMACHY by WFM-DOAS: year 2003 initial data set, Atmos. Chem. Phys., 5, 3313–3329, 2005b. 5390, 5391, 5392, 5393, 5394, 5395

Chahine, M., Barnet, C., Olsen, E. T., Chen, L., and Maddy, E.: On the determination of atmospheric minor gases by the method of vanishing partial derivatives with application to CO_2, Geophys. Res. Letts., 32, L22 803, doi:10.1029/2005GL024165, 2005. 5389

Chédin, A., Hollingsworth, A., Scott, N. A., Serrar, S., Crevoisier, C., and Armante, R.: Annual and seasonal variations of atmospheric CO_2, N_2O and CO concentrations retrieved from NOAA/TOVS satellite observations, Geophys. Res. Lett., 29(8), 1269, doi:10.1029/2001GL014082, 2002. 5389

Chédin, A., Serrar, S., Scott, N. A., Crevoisier, C., and Armante, R.: First global measurement of midtropospheric CO_2 from NOAA polar satellites: Tropical zone, J. Geophys. Res., 108(D18), 4581, doi:10.1029/2003JD003439, 2003. 5389

Chevallier, F., Engelen, R. J., and Peylin, P.: The contribution of AIRS data to the estimation of CO_2 sources and sinks, Geophys. Res. Lett., 32, L23 801, doi:10.1029/2005GL024229, 2005. 5389

Coldewey-Egbers, M., Weber, M., Lamsal, L. N., de Beek, R., Buchwitz, M., and Burrows, J. P.: Total ozone retrieval from GOME UV spectral data using the weighting function DOAS approach, Atmos. Chem. Phys., 5, 1015–1025, 2005. 5392

Crisp, D., Atlas, R., Bréon, F.-M., Brown, L., Burrows, J., Ciais, P., Connor, B., Doney, S., Fung, I., Jacob, D., Miller, C., O'Brien, D., Pawson, S., Randerson, J., Rayner, P., Salawitch, R., Sander, S., Sen, B., Stephens, G., Tans, P., Toon, G., Wennberg, P., Wofsy, S., Yung, Y., Kuang, Z., Chudasama, B., Sprague, G., Wiess, B., Pollock, R., Kenyon, D., and Schroll, S.: The Orbiting Carbon Observatory (OCO) mission, Adv. Space Res., 34(4), 700–709, 2004. 5390

Dils, B., De Mazire, M., Blumenstock, T., Buchwitz, M., de Beek, R., Demoulin, P., Duchatelet, P., Fast, H., Frankenberg, C., Gloudemans, A., Griffith, D., Jones, N., Kerzenmacher, T.,

Kramer, I., Mahieu, E., Mellqvist, J., Mittermeier, R. L., Notholt, J., Rinsland, C. P., Schrijver, H., Smale, D., Strandberg, A., Straume, A. G., Stremme, W., Strong, K., Sussmann, R., Taylor, J., van den Broek, M., Wagner, T., Warneke, T., Wiacek, A., and Wood, S.: Comparisons between SCIAMACHY and ground-based FTIR data for total columns of CO, CH_4, CO_2 and N_2O, Atmos. Chem. Phys., 6, 1953–1976, 2006. 5390, 5395, 5397, 5410

Frankenberg, C., Platt, U., and Wagner, T.: Retrieval of CO from SCIAMACHY onboard ENVISAT: detection of strongly polluted areas and seasonal patterns in global CO abundances, Atmos. Chem. Phys., 5, 1639–1644, 2005. 5394

Friedlingstein, P., Dufresne, J.-L., Cox, P. M., and Rayner, P.: How positive is the feedback between climate change and the carbon cycle?, Tellus, 55B, 692–700, 2003. 5389

Grzegorski, M., Frankenberg, C., Platt, U., Sanghavi, S., Fournier, N., Stammes, P., and Wagner, T.: Application of the HICRU cloud algorithm on SCIAMACHY: design and intercomparision, Geophys. Res. Abstr., 7, 08 316, 2005. 5394

Gurney, K. R., Law, R. M., Denning, A. S., Rayner, P. J., Baker, D., Bousquet, P., Bruhwilerk, L., Chen, Y.-H., Ciais, P., Fan, S., Fung, I. Y., Gloor, M., Heimann, M., Higuchi, K., John, J., Maki, T., Maksyutov, S., Masariek, K., Peylin, P., Pratherkk, M., Pakkk, B. C., Randerson, J., Sarmiento, J., Taguchi, S., Takahashi, T., and Yuen, C.-W.: Towards robust regional estimates of sources and sinks using atmospheric transport models, Nature, 415, 626–630, 2002. 5389

Heimann, M. and Körner, S.: The Global Atmospheric Tracer Model TM3, Model Description and Users Manual Release 3.8a, Tech. Rep. 5, Max Planck Institute for Biogeochemistry (MPI-BGC), Jena, Germany, 2003. 5398

Houweling, S., Brëon, F.-M., Aben, I., Rödenbeck, C., Gloor, M., Heimann, M., and Ciais, P.: Inverse modeling of CO_2 sources and sinks using satellite data: a synthetic inter-comparison of measurement techniques and their performance as a function of space and time, Atmos. Chem. Phys., 4, 523–538, 2004. 5389

Houweling, S., Hartmann, W., Aben, I., Schrijver, H., Skidmore, J., Roelofs, G.-J., and Brëon, F.-M.: Evidence of systematic errors in SCIAMACHY-observed CO_2 due to aerosols, Atmos. Chem. Phys., 5, 3003–3013, 2005. 5393, 5400, 5401

Intergovernmental Panel on Climate Change: Climate Change 2001: Synthesis Report: Third Assessment Report of the Intergovernmental Panel on Climate Change, Cambridge University Press, New York, 2001. 5389

Kleipool, Q.: Algorithm Specification for Dark Signal Determination, Tech. rep., SRON-SCIA-30

PhE-RP-009, SRON, 2003a. 5394
Kleipool, Q.: Recalculation of OPTEC5 Non-Linearity, Report containing the NL correction to be implemented in the data processor, Tech. rep. SRON-SCIA-PhE-RP-013, SRON, 2003b. 5394
Kneizys, F. X., Abreu, L. W., Anderson, G. P., Shettle, E. P., Chetwynd, J. H., Shettle, E. P., Berk, A., Bernstein, L., Robertson, D., Acharya, P., Rothman, L., Selby, J. E. A., Allery, W. O., and Clough, S. A.: The MODTRAN 2/3 report and LOWTRAN 7 model, Tech. rep., Philips Laboratory, Hanscom AFB, 1996. 5394
Krijger, J. M., Aben, I., and Schrijver, H.: Distinction between clouds and ice/snow covered surfaces in the identification of cloud-free observations using SCIAMACHY PMDs, Atmos. Chem. Phys., 5, 2279–2738, 2005. 5394
McClatchey, R. A., Fenn, R. W., Selby, J. E. A., Volz, F. E., and Garing, J. S.: Optical properties of the atmosphere, 3rd ed., Environ. Res. Pap. 411, AFCRL-72-0497, Air Force Cambridge Res. Lab., Bedford, Mass., 1972. 5413
Murphy, C., Bell, W., Woods, P., Demoulin, P., Galle, B., Mellqvist, J., Arlander, W., Notholt, J., Goldman, A., Toon, G., Blavier, J.-F., Sen, B., Coffey, M., Hannigan, J., Mankin, W., Jones, N., Griffith, D., Meier, A., Blumenstock, T., Fast, H., Mittermeier, R., and Makino, Y.: Validation of NDSC Measurements of Ozone, Reservoir Compounds and Dynamical Tracers: Results of a Series of Side-by-Side Instrument Intercomparisons, NDSC 2001 Symposium, Arcachon, France, 24–27 September 2001. 5395
Nöel, S., Buchwitz, M., and Burrows, J. P.: First retrieval of global water vapour column amounts from SCIAMACHY, Atmos. Chem. Phys., 4, 111–125, 2004. 5392
Olivier, J. G. J. and Berdowski, J. J. M.: Global emissions sources and sinks, in: The Climate System, edited by: Berdowski, J., Guicherit, R., and Heij, B. J., 33–78 pp., A. Balkema Publishers/Swets & Zeitlinger Publishers, Lisse, The Netherlands., 2001. 5398
Platt, U.: Differential optical absorption spectroscopy (DOAS), in Air Monitoring by Spectroscopic Techniques, John Wiley, New York, 1994. 5391
Rayner, P. J. and O'Brien, D. M.: The utility of remotely sensed CO_2 concetration data in surface source inversions, Geophys. Res. Lett., 28, 175–178, 2001. 5389
Rothman, L., Jacquemart, D., Barbe, A., Benner, C. D., Birk, M., Brown, L. R., Carleer, M. R., Chackerian Jr., C., Chance, K., Coudert, L. H., Dana, V., Devi, V. M., Flaud, J.-M., Gamache, R. R., Goldman, A., Hartmann, J.-M., Jucks, J. W., Maki, A. G., Mandin, J.-Y., Massie, S. T., Orphal, J., Perrin, A., Rinsland, C. P., Smith, M., Tennyson, J., Tolchenov, R. N.,

Toth, R. A., Vander Auwera, J., Varanasi, P., and Wagner, G.: The *HITRAN* 2004 molecular spectroscopic database, J. Quant. Spectrosc. Radiat. Transfer, 96, 193–204, 2005. 5394

Rozanov, V. V., Buchwitz, M., Eichmann, K. U., de Beek, R., and Burrows, J. P.: SCIATRAN - a new radiative transfer model for geophysical applications in the 240–2400 nm spectral region: The pseudo-spherical version, presented at COSPAR 2000, Adv. Space Res., 29(11), 1831–1835, 2002. 5393

Sabine, C. L., Freely, R. A., Gruber, N., Key, R. M., Lee, K., Bullister, J. L., Wanninkhof, R., Wong, C. S., Wallace, D. W. R., Tilbrook, B., Millero, F. J., Peng, T.-H., Kozyr, A., Ono, T., and Roso, A. F.: The Oceanic Sink for Anthropogenic CO_2, Science, 305, 367–371, 2004. 5389

Siegenthaler, U., Stocker, T. F., Monnin, E., Lüthi, D., Schwander, J., Stauffer, B., Raynaud, D., Barnola, J.-M., Fischer, H., and Valérie Masson-Delmotte, J. J.: Stable Carbon CycleClimate Relationship During the Late Pleistocene, Science, 310, 1313–1317, 2005. 5389

Takahashi, T., Sutherland, S. C., Sweeney, C., Poisson, A., Metzl, N., Tilbrook, B., Bates, N., Wanninkhof, R., Feely, R. A., Sabine, C., Olafsson, J., and Nojiri, Y.: Global sea-air CO_2 flux based on climatological surface ocean pCO_2, and seasonal biological and temperature effects, Deep-Sea Res. II, 49, 1601–1622, 2002. 5398

Thornton, P. E., Running, S. W., and Hunt, E. R.: Biome-BGC: Terrestrial Ecosystem Process Model, Version 4.1.1, Model product. Available on-line (http://www.daac.ornl.gov) from Oak Ridge National Laboratory Distributed Active Archive Center, Oak Ridge, Tennessee, USA, 2005. 5398

van der Werf, G. R., Randerson, J. T., Collatz, G. J., and Giglio, L.: Carbon emissions from fires in tropical and subtropical ecosystems, Global Change Biology, 9, 547–562, 2003. 5398

Wennberg, P., Washenfelder, R., Yavin, Y., Toon, G., Blavier, J.-F., Salawitch, R., Connor, B., Sherlock, V., Wood, S., Notholt, J., Warneke, T., Griffith, D., Deutscher, N., Bryant, G., and Jones, N.: The Total Carbon Column Observing Network (TCCON), AGU, 86(52), Fall Meet. Suppl., Abstract A12D-01, 2005. 5390

Yang, Z., Toon, G. C., Margolis, J. S., and Wennberg, P. O.: Atmospheric CO_2 retrieved from ground-based near IR solar spectra, Geophys. Res. Lett., 29(9), 1339, doi:10.1029/2001GL014537, 2002. 5394

Table 1. Summary of the FSI retrievals plus the WFM-DOAS results presented in Dils et al. (2006) (labeled WFM-DOAS$_{IUP}$, retrieved by Michael Buchwitz and Rudiger de Beek, IUP/IFE Bremen). Analysis of the TM3 model data (Sect. 5) is also included. Shown, for both the large and small grids, are the 2003 mean bias B_{year}, its standard deviation σ_{Bias} and relative scatter σ_{scat} each with respect to the 3rd order polynomial fit. The scatter of the FTIR data is 1.3%. The top three rows refer to the CO_2 VCDs, whilst the final two rows indicate the FSI retrievals and TM3 model VMR data.

Retrieval Algorithm/ Model	Number of observations	Large grid			Small grid		
		B_{year} [%]	σ_{Bias} [%]	σ_{scat} [%]	B_{year} [%]	σ_{Bias} [%]	σ_{scat} [%]
FSI	5150	−4.1	3.0	0.8	−4.0	3.0	1.3
TM3 Model	5150	−1.8	2.0	0.4	−1.9	2.0	0.7
WFM-DOAS$_{IUP}$	2232	−12.0	7.4	5.5	−11.3	5.7	6.7
FSI	5150	−4.3	3.0	1.5	−4.3	3.0	2.7
TM3 Model	5150	−2.0	0.9	<0.1	−2.0	0.9	<0.1

Table 2. Summary of the FSI retrievals and TM3 model comparisons. Note, "SCA" refers to the Seasonal Cycle Amplitude and the "Mean Correlation" refers to the average correlation between the data sets. Typically SCIAMACHY under estimates the yearly mean by approximately 2%, whilst the average difference between observation and model is 1–3% depending on the region.

Region	Yearly mean [ppmv]		SCA [ppmv]		Difference [ppmv]		Time series correlation	Mean correlation
	FSI	TM3	FSI	TM3	Mean	1σ	[–]	[–]
Gobi Desert	374.0	377.3	10.1	4.9	3.3	6.9	0.95	0.16
North America	371.6	377.5	15.4	7.0	6.0	7.9	0.67	0.12
Siberia	371.2	377.5	20.7	7.9	7.3	7.6	0.75	0.15
Western Europe	367.5	378.1	13.5	5.7	10.7	8.6	0.47	0.16

Table 3. The FSI retrieval errors over the four selected scenes (Fig. 4).

Region	Mean Retrieval Error [%]	1σ [%]	Mean RMS [%]
Gobi Desert	1.9	0.4	0.1
North American	2.9	0.8	0.3
Siberia	2.7	0.6	0.3
Western Europe	2.6	0.7	0.2

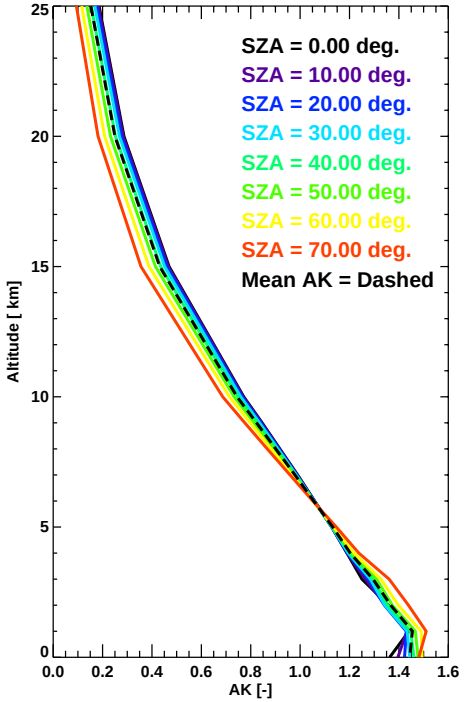

Fig. 1. Averaging kernels of the FSI algorithm for the retrieval of CO_2 from SCIAMACHY NIR measurements, for various solar zenith angles (SZA), using the fitting window 1561.03–1585.39 nm and albedo=0.2. These averaging kernels have been generated by perturbing the US Standard atmosphere (McClatchey et al., 1972) by 10 ppmv, at 1 km intervals below 10 km and 5 km steps above 10 km. The average kernels have been calculated using the formula $AK(z)=(V^{rp}-V^{tu})/(V^{tp}-V^{tu})$, where V^{rp} is the retrieved perturbed vertical column density, V^{tp} the true perturbed column, V^{tu} the true unperturbed column and z is the altitude (see Buchwitz and Burrows, 2004). The mean averaging kernel, applied to the TM3 model data (see Sect. 5) is also plotted (black dashed).

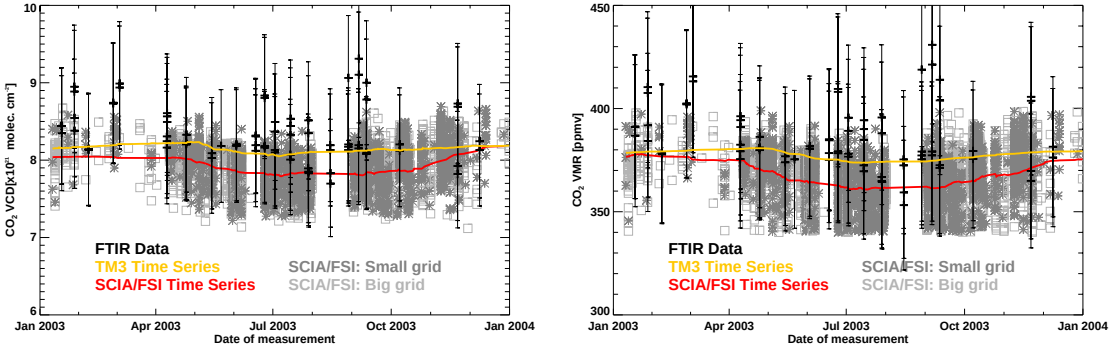

Fig. 2. **(a)** Left panel: The ground based FTIR CO_2VCDs (±9.8% error, black crosses) and the FSI retrieved VCDs grouped as a large grid (within ±10.0° longitude and ±2.5° latitude, light grey squares) and a small grid (within ±5.0° longitude and ±2.5° latitude, dark grey stars) relative to the Egbert station. Red line: A 31 point box-car average of the (daily averaged) FSI CO_2 VCDs. Orange line: A 31 point box-car average of the (daily averaged) TM3 model data (see Sect. 5) interpolated onto the Egbert location. **(b)** Right panel: As left but for the VMRS (i.e. VCDs normalized by the surface pressure).

ACPD
6, 5387–5425, 2006

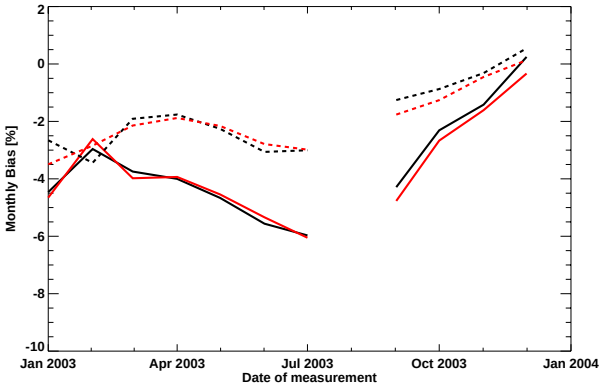

Fig. 3. The average monthly biases, in percent, for both the FSI retrievals (solid lines) and the TM3 model (dashed lines) calculated for the CO_2 VMRs (red) and VCDs (black).

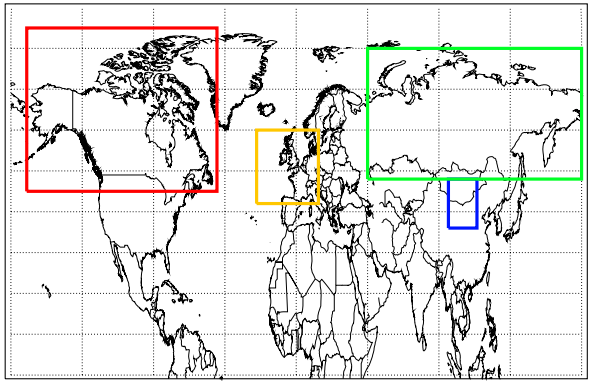

Fig. 4. The scenes used in the TM3 model comparisons: North American (red), Western Europe (Orange), Siberia (green) and the Gobi Desert (blue).

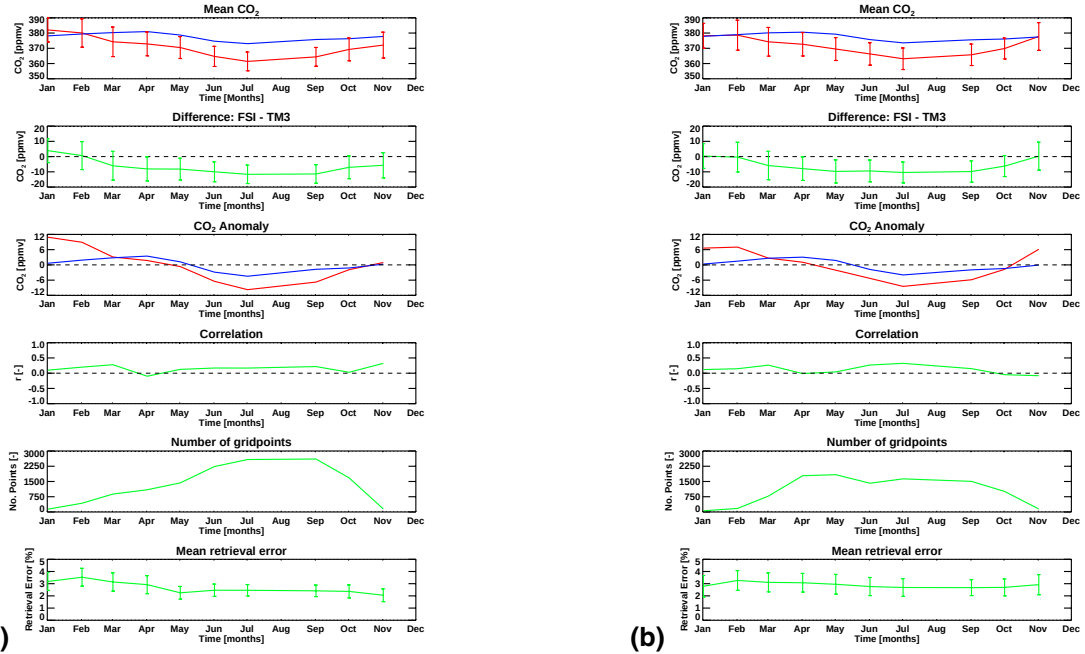

Fig. 5. Comparisons between the TM3 model data (blue lines) and the FSI retrieved CO_2 VMRs (red lines) for the **(a)** Siberian (left) and **(b)** North American (right) regions for the year 2003. Top panels: The mean CO_2 VMR of each scene. The error bars on the FSI data represent the 1 σ standard deviation of the mean. Second panels: The mean difference between the FSI columns and the TM3 data (equivalent to the difference between the monthly averages). The error bars represent the 1σ standard deviation of this difference. Third panels: The CO_2 anomaly (i.e. monthly averages minus the yearly mean). Fourth panels: The correlation coefficient between the two data sets. Fifth panels: The number of TM3 grid points used in the calculation of the scene means. Bottom panels: The mean FSI retrieval error of the observed CO_2 VMRs with the 1 σ standard deviation, which is consistently less than 1%. Note, at the time of processing, SCIAMACHY data for August was not available and that for December there was not enough valid FSI retrievals to perform a sensible comparison.

ACPD
6, 5387–5425, 2006

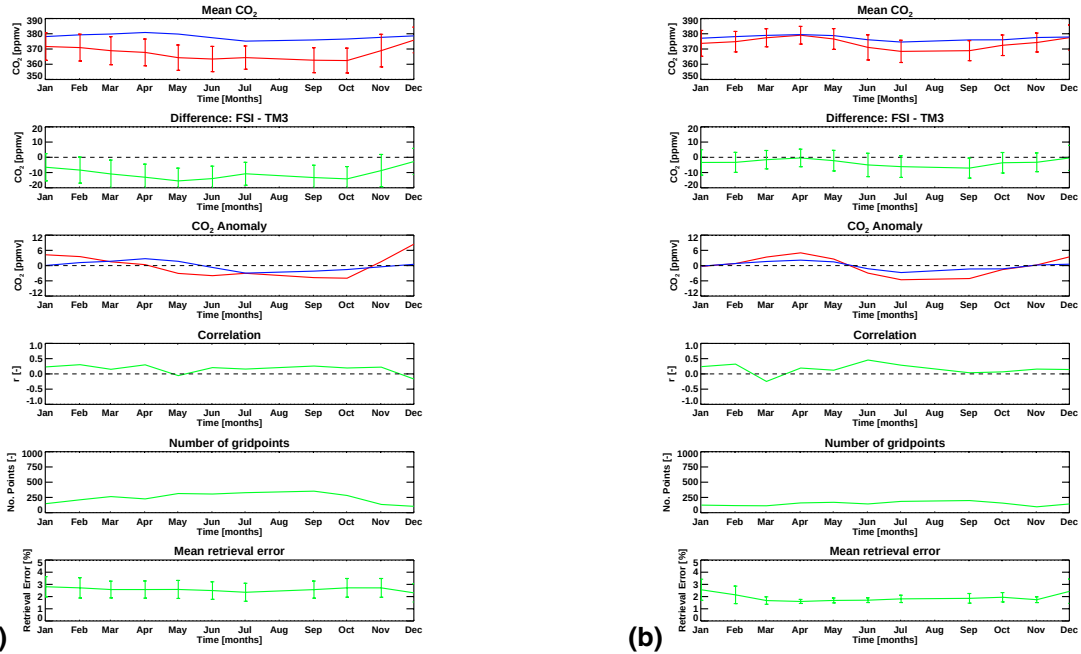

(a) **(b)**

Fig. 6. As Fig. 5 but for the **(a)** Western Europe (left) and **(b)** Gobi Desert (right) regions for the year 2003.

ACPD
6, 5387–5425, 2006

EGU

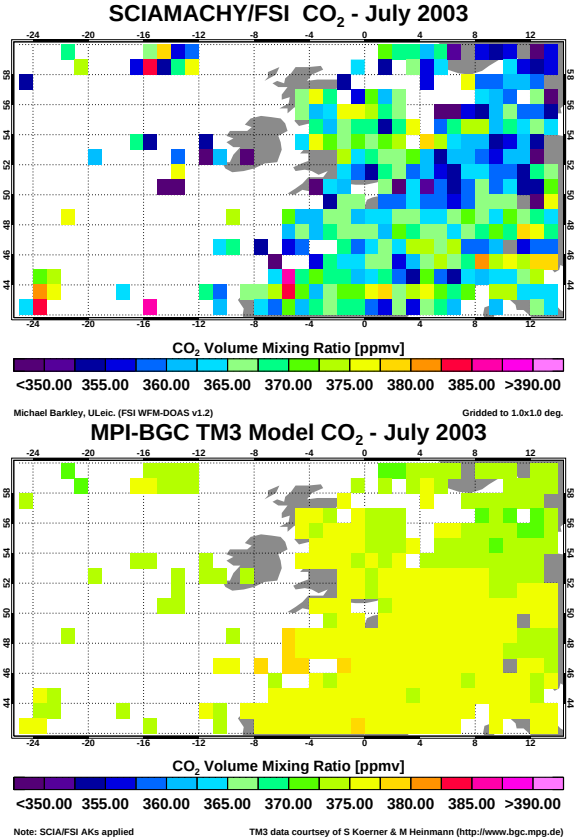

Fig. 7. Top: The FSI retrieved CO_2 VMRs over the Western Europe for the July 2003. For this region only, pixels over the oceans were also processed. Bottom: The corresponding TM3 model CO_2 field. Both model and SCIAMACHY observations agree on lower concentrations over the Netherlands, Denmark and north Germany despite an offset between the absolute values.

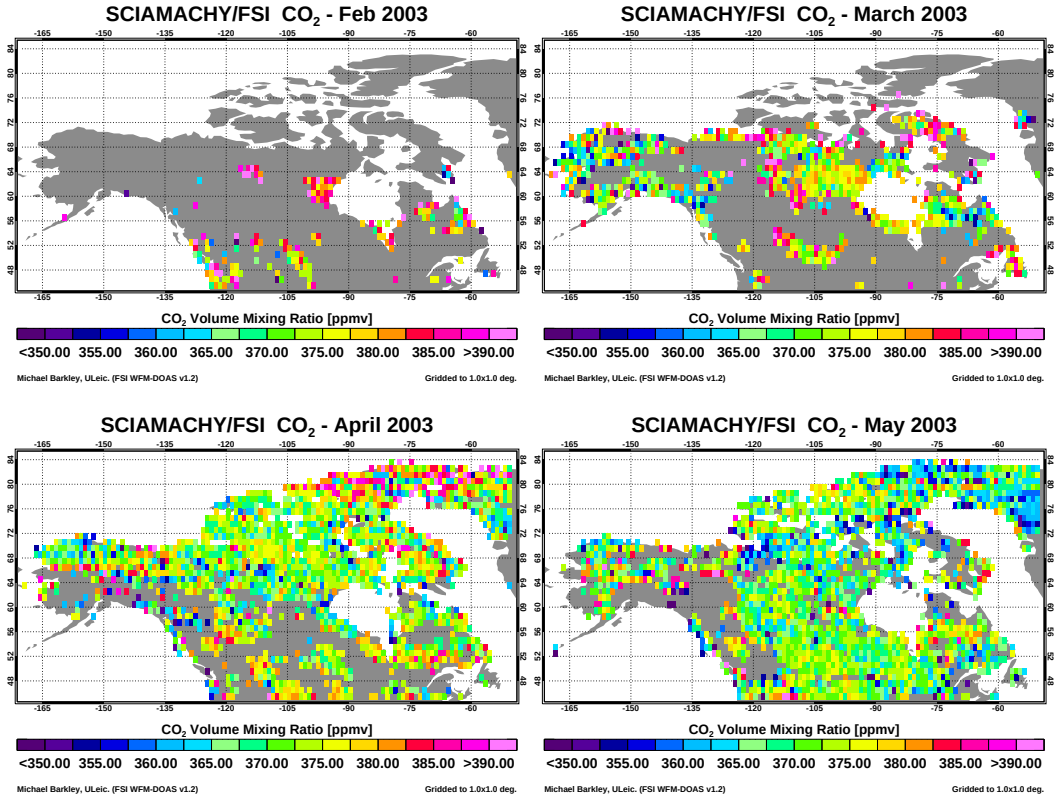

Fig. 8. The SCIAMACHY/FSI monthly scene averages over North America for 2003, on a 1°×1° grid.

ACPD
6, 5387–5425, 2006

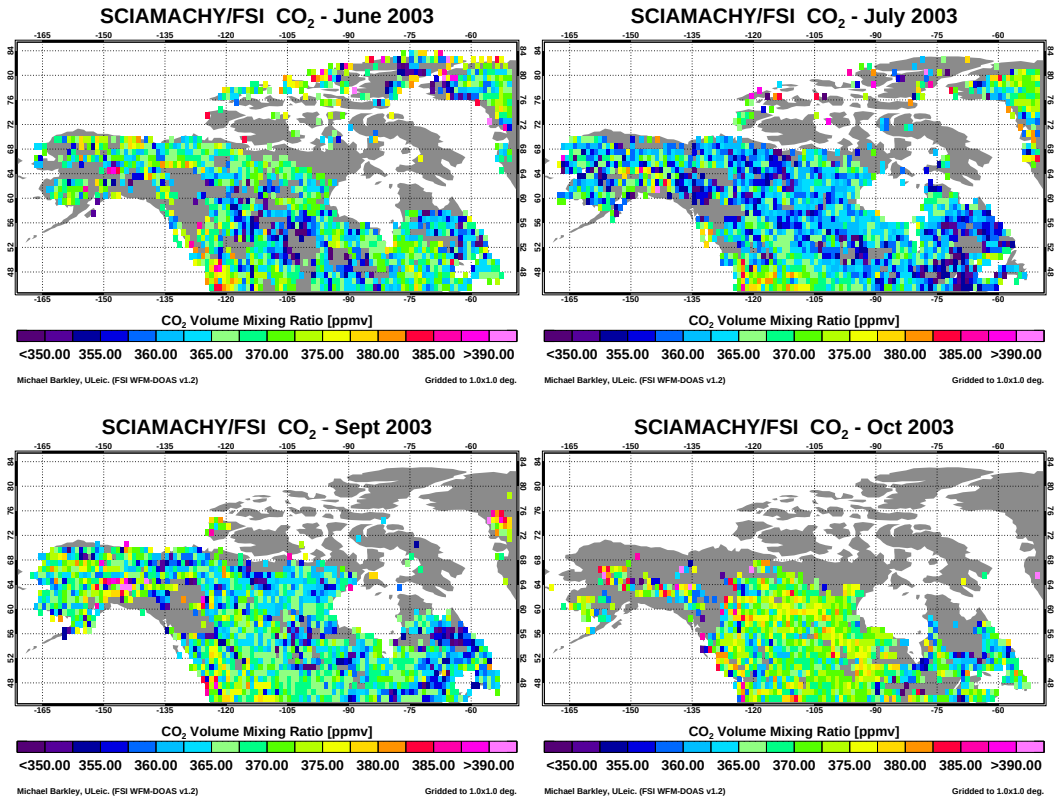

Fig. 8. Continued.

ACPD
6, 5387–5425, 2006

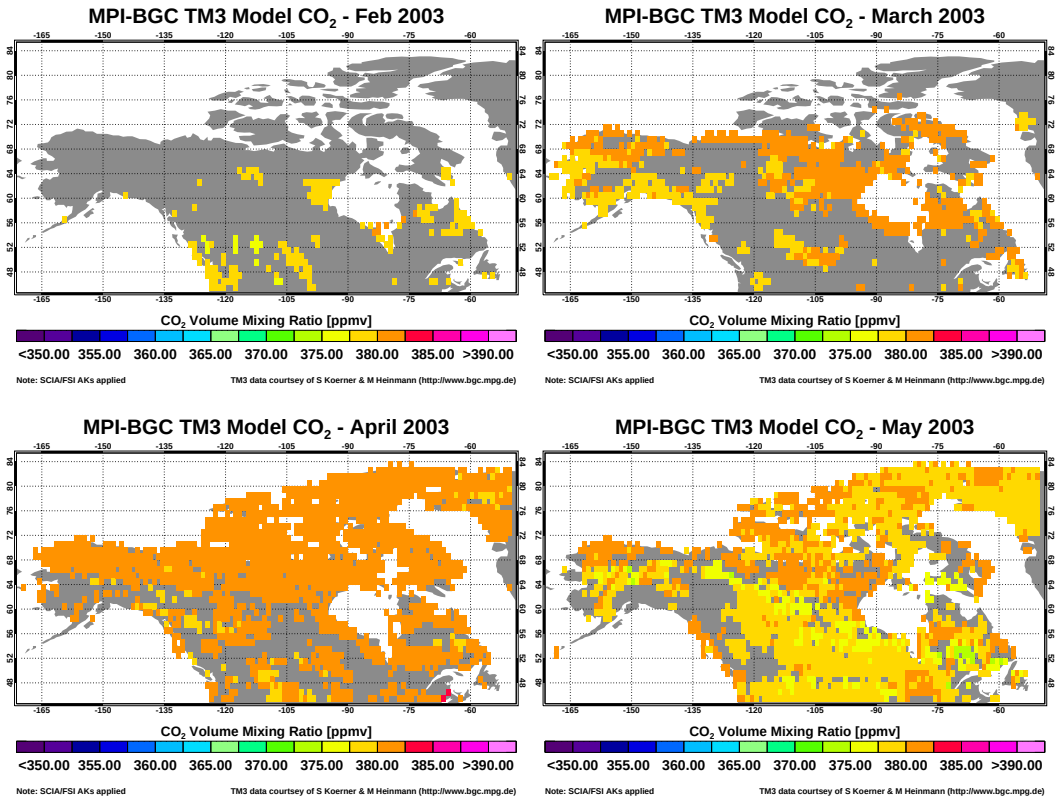

Fig. 9. The TM3 model monthly scene averages over North America for 2003, on a 1°×1° grid.

ACPD
6, 5387–5425, 2006

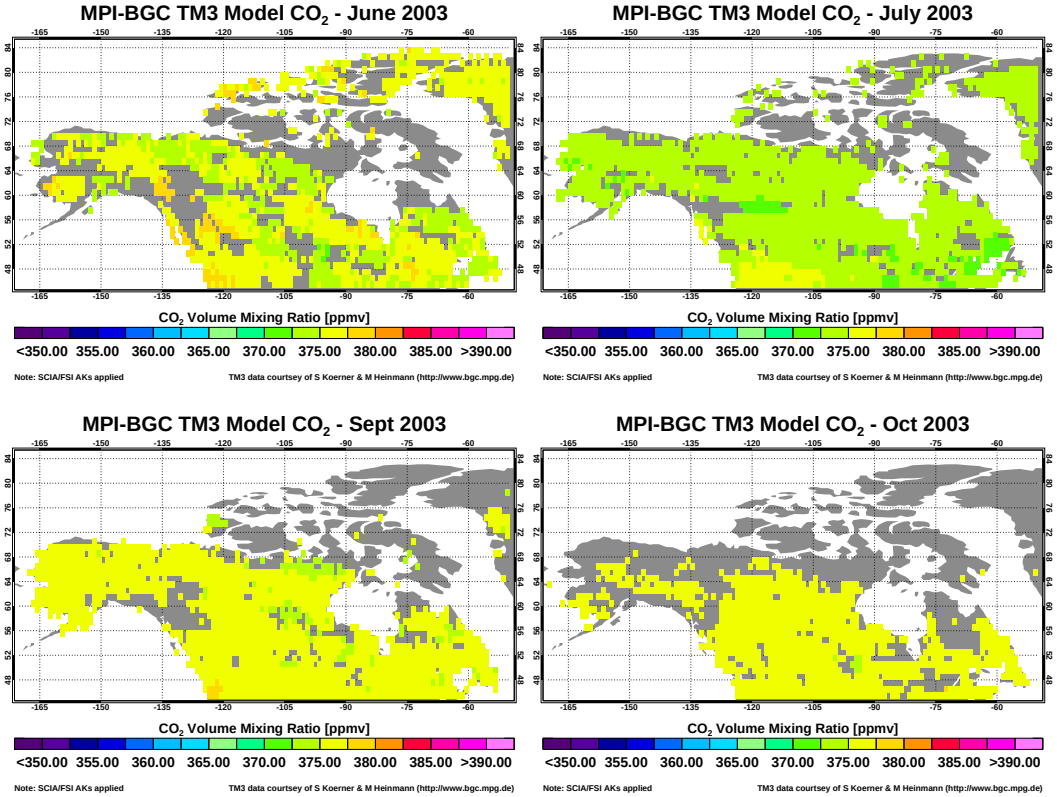

Fig. 9. Continued.

ACPD
6, 5387–5425, 2006

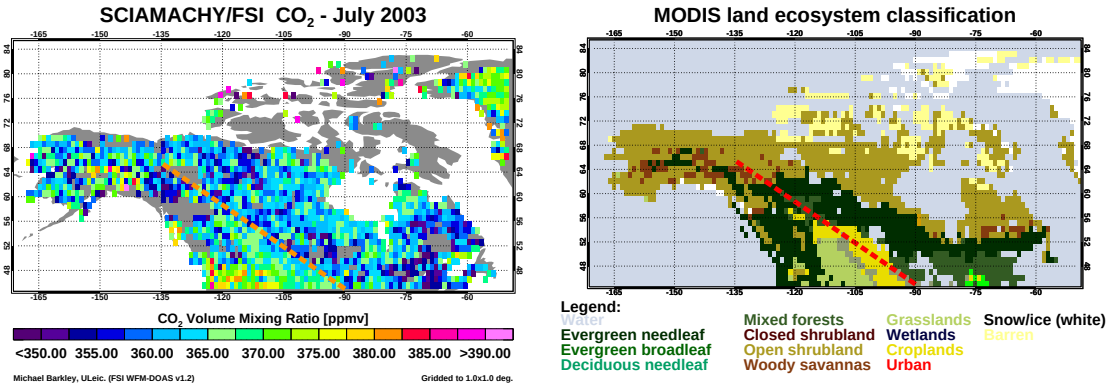

Fig. 10. SCIAMACHY CO_2 observations over North America for July 2003 (left panel) with a map of the land vegetation cover over this scene (right panel). The red dashed line divides areas of low CO_2 concentrations (to the right) and higher values (to the left) which corresponds to a transition from vegetation type from evergreen needle leaf and mixed forests to land covered by crops and large grass plains. The vegetation map is taken from the Land Ecosystem Classification Product which is a static map generated from the official MODIS land ecosystem classification data set, MOD12Q1 for year 2000, day 289 data (15 October 2000) (see http://modis-atmos.gsfc.nasa.gov/ECOSYSTEM/index.html).

ACPD
6, 5387–5425, 2006

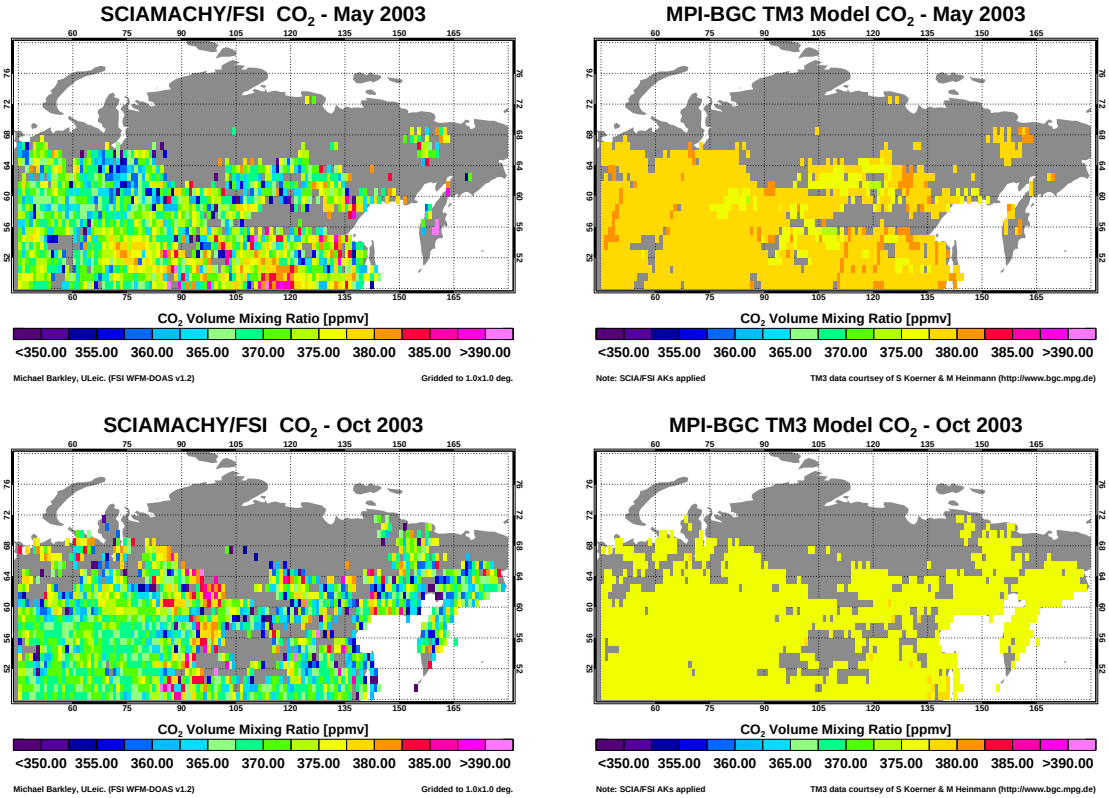

Fig. 11. The monthly scene averages of the FSI CO_2 retrievals (left panels) and TM3 model (right panels), over Siberia for May (top) and October (bottom), 2003.

ACPD
6, 5387–5425, 2006